Macromolecular Research, Vol. 19, No. 7, pp 739-748 (2011)
DOI 10.1007/s13233-011-0706-2

A pH-Sensitive Composite Hydrogel Based on Sodium Alginate and Medical Stone: Synthesis, Swelling, and Heavy Metal Ions Adsorption Properties

Tianpeng Gao[1,2,3], Wenbo Wang[1], and Aiqin Wang*[,1]

[1]*Center for Eco-material and Green Chemistry, Lanzhou Institute of Chemical Physics, Chinese Academy of Sciences, Lanzhou 730000, P.R. China*
[2]*Graduate University of the Chinese Academy of Sciences, Beijing 100049, P.R. China*
[3]*School of Chemistry and Environmental Science, Lanzhou City University, Lanzhou 730000, P.R. China*

Received December 15, 2010; Revised February 7, 2011; Accepted February 8, 2011

Abstract: New pH-sensitive composite hydrogels were synthesized by free-radical graft copolymerization among sodium alginate (NaAlg), sodium acrylate (NaA), and medical stone (MS). Fourier transform infrared spectroscopy (FTIR), field emission scanning electron microscopy (FESEM), tronsmission electron microscopy (TEM), and thermogravimetric analysis (TGA) analyses confirmed that NaA was grafted onto the NaAlg chains and MS participate in polymerization by its active silanol groups, and the surface morphologies and thermal stability was clearly improved after incorporating MS. The swelling capacity and rate of the hydrogel were clearly enhanced by introducing MS, and the intriguing deswelling in gelatin solution and "overflowing" behaviors in dimethyl sulfoxide (DMSO) and glycerin solutions were observed. In addition, the composite hydrogels exhibited excellent adsorption capacity on heavy metal ions, which enhanced the adsorption of Ni^{2+}, Cu^{2+}, Zn^{2+} and Cd^{2+} ions by 10.4, 8.0, 23.0, and 14.3 fold compared to active carbon (AC), and by 17.3, 16.0, 38.3 and 23.8 fold compared to MS, respectively. The biopolymer-based composite hydrogel can be used as a potential water-saving material and candidate of AC for heavy metal removal.

Keywords: composite hydrogel, sodium alginate, medical stone, swelling, adsorption, pH-sensitivity.

Introduction

Hydrogels are crosslinked hydrophilic functional polymer materials with special three-dimensional network structure and various functional groups, which can swell in aqueous solution or response to external stimulation, but do not disintegrate or dissolve.[1] By virtue of the unique advantages, hydrogels become one of the upcoming classes of polymer-based materials and have found extensive applications in many fields, such as water-saving materials for agriculture,[2,3] hygienic products,[4] drug-delivery systems,[5-7] wastewater treatment,[8-12] dehydrating agent,[13] tissue engineering,[14] and biosensor,[15] etc. Thus far, numerous hydrogel materials have been developed by using various raw materials and methods. Among them, the design of environmentally friendly hydrogel materials based on naturally occurred materials, such as polysaccharide and clay minerals, has especially been focused due to the increasing public concerns on the environmental protection topic and the safety of materials.[16,17] Polysaccharides including starch,[18] cellulose,[19] guar gum,[20] κ-carrageenan,[21] chitosan,[22] cashew gum,[23] alginate,[24] and pectin[2,25] etc. have become the preferred and promising matrix for preparing hydrogel because their renewable, low-cost, non-toxic, biodegradable and biocompatible superiors and clay minerals can act as effective fillers to adjust the swelling degree of the hydrogel materials. The composite of polysaccharides and inorganic clay minerals showed surprising performance superior to their individual components and has been honored as the materials "in greening the 21st century materials world".[16]

Sodium alginate (NaAlg) is a renewable anionic linear natural polysaccharide extracted from marine algae or produced by bacteria. NaAlg is composed of poly-β-1,4-D-mannuronic acid (M units) and α-1,4-L-glucuronic acid (G units) in varying proportions, and so it is renewable, water soluble, odourless, non-toxic and biodegradable. Also, NaAlg has higher reactive activities and can be easily modified by ionically crosslinking,[26] grafting copolymerization,[27] polymer blending[28] or chemical compounding with other components[29] to derive new hydrogel materials. Among these methods, grafting copolymerization with vinyl monomers and compounding other components can introduce functional groups on the NaAlg backbone most efficiently, which showed great potential to produce NaAlg-based functional materials

*Corresponding Author. E-mail: aqwang@licp.cas.cn

and extend the application domains.

Medical Stone (MS) is a special igneous rock composed of silicic acid, alumina oxide and more than 50 kinds of macro, micro and trace elements. The main chemical configuration of MS is aluminum metasilicate (feldspar) including $KAlSi_3O_8$, $NaAlSi_3O_8$, $CaAl_2Si_2O_8$, $MgAl_2Si_2O_8$ and $FeAl_2Si_2O_8$, etc. In its structure, silica (SiO_2) has regular tetrahedron with a [SiO_4] configuration, and shows a three-dimensional stereo-structure in which aluminum coordinates through oxo-bridging. MS has excellent multi-component characteristic, biological activity and safety, and so it has been widely applied in food science, medicine, daily chemical industry, environmental sanitation and mineral water, etc..[30] However, these applications of MS are still limited in the direct usage of raw mineral powder, and little research focused on the development of composite materials based on MS. Hence, the graft copolymerization of NaAlg and vinyl monomers and then compounding with MS to fabricate new eco-friendly composite hydrogels has exhibited great prospects, and the structure and swelling properties of the hydrogels can also be simultaneously improved.

On basis of above description, in this paper, we prepared a new NaAlg-*g*-PNaA/MS composite hydrogel by a facile solution free-radical polymerization reaction among NaAlg, NaA and MS. The structure, morphologies and thermal stability of the developed composite were characterized by Fourier transform infrared spectra (FTIR), Field emission scanning microscopy (FESEM), transmission electron micrographs (TEM) and thermogravimetric analysis (TGA) techniques. The swelling capacity and swelling rate of the composite hydrogel and the effect of various polymer solutions, salt solutions, pH solutions and hydrophilic organic solvents on the swelling properties were investigated systematically. In addition, the adsorption properties of the composite hydrogel on Ni^{2+}, Cu^{2+}, Zn^{2+} and Cd^{2+} ions were evaluated.

Experimental

Materials. NaAlg with a kinetic viscosity of 20 cp (1.0% aqueous solution) at 20 ºC was from Shanghai chemical reagents Co., (Shanghai, China). Acrylic acid (AA, chemically pure, Shanghai Shanpu Chemical Factory, Shanghai, China) was distilled under reduced pressure before use. Medical stone (MS) micro-powder (Chinese M-Stone Development Co., Ltd, NaiMan, Inner Mongolia, China) was milled and passed through a 320-mesh screen (< 46 μm) prior to use, and the main chemical composition is SiO_2, 68.89%; Al_2O_3, 14.06%; Fe_2O_3, 3.61%; K_2O, 3.18%; Na_2O, 4.86%; CaO, 1.33%; MgO, 2.59%. Active carbon (AC) from coconut shell was purchased from Fuzhou Yihuan Carbon Co., LTD (Fuzhou, China). Ammonium persulfate (APS, analytical grade, Xi'an Chemical Reagent Factory, China) and *N*,*N*-methylene-*bis*-acrylamide (MBA, chemically pure, Shanghai Chemical Reagent Corp., China) was used as received. Cetyltrimethylammonium bromide (CTAB) was supplied by Beijing Chemical Reagents Company (Beijing, China). All other chemicals were of analytical reagent grade and solutions were prepared with purified water.

Preparation of NaAlg-*g*-PNaA/MS Composite Hydrogels. NaAlg (1.04 g) was dissolved in 30 mL of distilled water at 60 ºC in a 250 mL four-necked flask equipped with a mechanical stirrer, a thermometer, a reflux condenser and a nitrogen line to obtain a transparent solution. Afterward, 5 mL of the aqueous solution of the initiator APS (72 mg) was added dropwise to the reaction flask under continuous stirring, and kept at 60 ºC for 10 min to generate radicals. 7.2 g of AA was pre-neutralized using 8.0 mL of 8.5 M NaOH solution, and then crosslinker MBA (21.6 mg) and calculated amount of MS powder (0, 0.44, 0.93, 2.08, 3.57 and 5.57 g, corresponded to the sample codes MS0, MS5, MS10, MS20 and MS30, respectively) were added under magnetic stirring to form a uniform dispersion. After cooling the reactant to 50 ºC, the dispersion was added to the reaction flask, and the temperature was gradually raised to 70 ºC and kept for 3 h to complete polymerization. Continuous purging of nitrogen was used throughout the reaction period. After being fully washed with distilled water, the obtained gel products were dried to a constant mass at 70 ºC, ground and passed through a 40-80 mesh sieve (180~380 μm).

Measurements of Swelling Capacity and Swelling Kinetics. Dry sample (about 0.05 g, m_1) with the size of 180~380 μm was adequately contacted with excessive aqueous solution at room temperature for 4 h, until a swelling equilibrium was reached. The swollen samples were separated by a 100-mesh screen and then drain on the sieve for 10 min to remove the redundant water. After weighed the swollen samples (m_{2t}) at time t, the water absorption of the composite hydrogel at time t (Q_t) was calculated using eq. (1).

$$Q_t = (m_{2t} - m_1)/m_1 \quad (1)$$

At equilibrium, Q_t=Q_{eq} (g/g) and m_{2t}=m_∞. Q_{eq} (g/g) is the equilibrium water absorption calculated as grams of water per gram of sample, which are averages of three measurements; m_∞ (g) is the weights of the water-swollen sample at equilibrium state.

Kinetic swelling behaviors of the hydrogels in each aqueous solution were measured by the following procedure: 0.05 g samples were immersed in 200 mL of aqueous solution for a set period of time. Then, the swollen gels were filtered using a 100-mesh sieve, and the water absorption (Q_t) of hydrogels at a given time (t) can be measured by weighing the swollen and dry samples, and calculated according to eq. (1). In all cases three parallel samples were used and the averages are reported in this paper.

Evaluation of pH-Sensitive Properties. The solutions with pHs 2.0 and 7.4 were adjusted by 0.1 M HCl and NaOH solutions and the pH values were determined by a pH meter

(DELTA-320). The pH-reversibility of the composites was investigated in terms of their swelling and deswelling between pHs 2.0 and 7.4 solutions. Typically, the sample (0.05 g, 180~380 μm) was placed in a 100 mesh sieve and adequately contacted with pH 2.0 solution until achieving equilibrium. Then, the swollen samples were soaked in pH 7.4 solution for set time intervals. Finally, the swollen samples were filtered, weighed and then calculated the swelling capacity at a given moment according to the mass change of samples before and after swelling. The consecutive time interval is 15 min for each cycle, and the same procedure was repeated for five cycles. After every measurement, each solution was renewed.

Adsorption Equilibrium Experiments on Heavy Metal Ions. The heavy metal ions solutions (0.01 mol/L) were prepared by dissolving of $Ni(Ac)_2$, $Cu(Ac)_2$, $Zn(Ac)_2$ and $Cd(Ac)_2$ in distilled water, and the pH values were adjusted to 5.5 with dilute NaOH or HCl solution (0.1 mol/L). The equilibrium adsorption experiments were carried out on thermostatic shaker (THZ-98A) with a constant speed of 120 rpm. The adsorption properties of the activated carbon (AC), medical stone (MS) and the composite hydrogels were evaluated in the 25 mL of test solutions with 0.05 g of adsorbents at 30 °C for 4 h. At the end of the adsorption period, the solution was centrifuged for 10 min at 4,500 rpm. The initial concentrations and final concentrations of heavy metal ions in the solution were measured by EDTA titrimetric method using 0.002 mol/L EDTA solution as the standard solution and 0.5% xylenol orange solution as the indicator.

Characterizations. FTIR spectra were recorded on a Nicolet NEXUS FTIR spectrometer in 4000-400 cm^{-1} region using KBr pellets. The samples were immersed in 60 vol% ethanol solution for 24 h and then thoroughly dried before FTIR determination. The surface morphologies of the samples were examined using a JSM-6701F Field Emission Scanning Electron Microscope (JEOL) after coating the sample with gold film. Thermal stability of samples was studied on a Perkin-Elmer TGA-7 thermogravimetric analyzer (Perkin-Elmer Cetus Instruments, Norwalk, CT), with a temperature range of 25-700 °C at a heating rate of 10 °C/min using dry nitrogen purge at a flow rate of 50 mL/min. The samples were dried at 100 °C for 4 h to remove the absorbed water before determining TG curves. The transmission electron micrographs (TEM) were obtained using a JEM-2010 high-resolution transmission electron microscope (JEOL, Tokyo, Japan) at an acceleration voltage of 200 kV, the sample was ultrasonically dispersed in ethanol before observation.

Results and Discussion

FTIR Analysis. The FTIR spectra of NaAlg, MS0, MS10, and MS are shown in Figure 1. It can be noticed from Figure 1(a) that the characteristic absorption bands of NaAlg

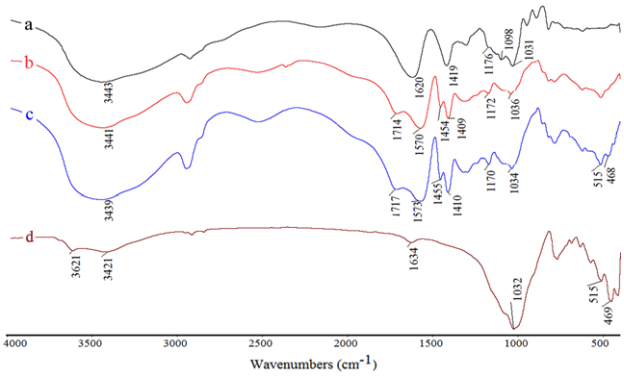

Figure 1. FTIR spectra of (a) NaAlg, (b) MS0, (c) MS10, and (d) MS.

at 1098 and 1031 cm^{-1} (stretching vibration of C-OH groups) were obviously weakened after reaction and the new absorption bands at 1714 cm^{-1} for MS0 and 1717 cm^{-1} for MS10 (the asymmetric stretching vibration of -COOH), at 1570 cm^{-1} for MS0 and 1573 cm^{-1} for MS10 (the asymmetric stretching of $-COO^-$), and at 1409~1455 cm^{-1} (symmetric stretching of $-COO^-$ groups) appeared in the spectra of the hydrogels (Figure 1(b) and (c)), indicating that NaA monomers were grafted onto the NaAlg backbone. As shown in Figure 1(d), the absorption band at 3621 cm^{-1} can be attributed to the (Si)O-H stretching vibration, which almost disappeared in the spectrum of MS10 (Figure 1(c)). The absorption band at 1032 cm^{-1} is due to the Si-O stretching vibration of MS, which shifted to 1034 cm^{-1} with a weakened intensity after polymerization reaction. In addition, the Si-O bending vibration of MS at 468 cm^{-1} can be observed in the spectrum of the composite hydrogel, but its intensity was obviously weakened. The above information reveals that MS participated in the graft copolymerization reaction through its active silanol groups.[31,32]

Thermal Analysis. The TGA technique was adopted to evaluate the thermal stability of the MS0 hydrogel and

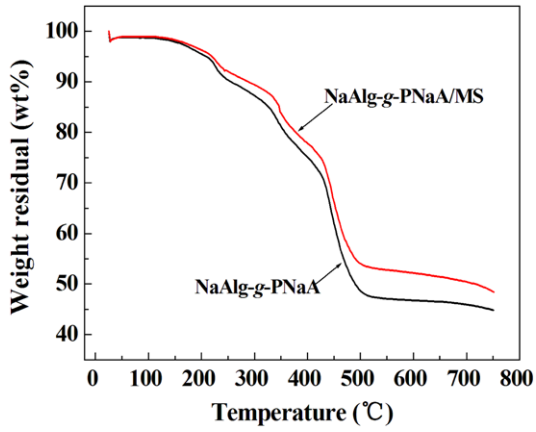

Figure 2. TGA curves of NaAlg-*g*-PNaA and NaAlg-*g*-PNaA/MS (10 wt%).

MS10 composite hydrogel (Figure 2). As can be seen, both the MS0 and MS10 showed three-stage main thermal decomposition, but the weight-loss rate of the MS10 is clearly slower than the MS0. The weight loss about 5.2 wt% below 219 ºC for MS0 and about 3.95 wt% below 215 ºC for MS10 can be ascribed to the removal of water absorbed. The successive weight loss about 8.2 wt% (219~318 ºC) for MS0 and about 8.1 wt% (215~337 ºC) for MS10 can be attributed to the lactonization or transglucosidation of NaAlg.[33] The successive weight loss about 14.4 wt% (318~429 ºC) for MS0 and about 13.5 wt% (337~435 ºC) for MS10 can be attributed to the breaking of C-O-C bonds in NaAlg chains and the formation of anhydride with the elimination of water molecule derived from the two neighboring carboxylic groups of the grafted PNaA chains.[34] The weight losses about 24.5 wt% between 429 and 485 ºC for MS0 and about 21.1 wt% between 435 and 489 ºC for MS10 are due to the breakage of main-chain scission and the destruction of crosslinked network structure. By comparison with MS0 matrix, MS10 composite hydrogel exhibited relatively higher decomposition temperature at each stage, slower weight-loss rate and lesser total weight loss, which indicate that the incorporation of MS improved the thermal stability of the hydrogel.

FESEM and TEM Morphologies. Introduction of MS can not only affect the composition of the composite hydrogel, but also its surface morphologies. Figure 3 depicts the FESEM micrographs of MS0, MS, MS10 and MS30. It can be observed that the MS0 hydrogel only shows a dense, smooth and non-porous surface structure, and MS shows a coarse and sheet surface structure (Figure 3(b)). After introducing MS into NaAlg-*g*-PNaA matrix, the surface roughness of the hydrogel was obviously improved, and some pores and gap was observed (Figure 3(c)). This indicates that introduction of moderate amount of MS contributes to improve the surface structure of the hydrogel. It can also be observed that the surface roughness of the composite increased with increasing the content of MS (Figure 3(d)). Moreover, this observation gives a direct revelation that MS led to a uniform dispersion and almost embedded within the MS0 matrix without the flocculation of MS particles, and a homogeneous composite structure was formed.

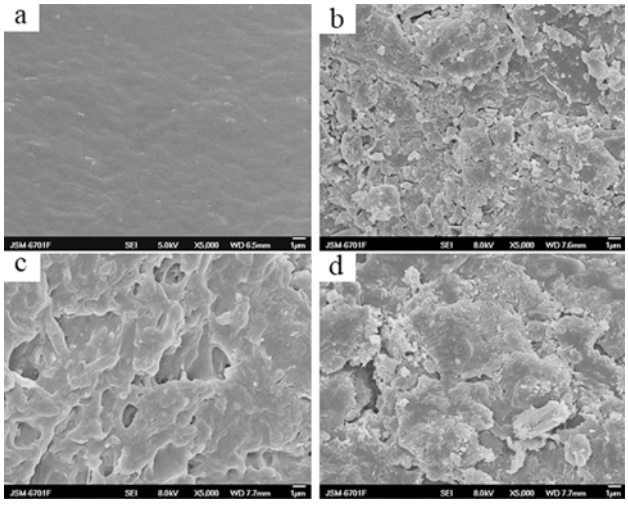

Figure 3. FESEM micrographs of (a) MS0, (b) MS, (c) MS10, and (d) MS30.

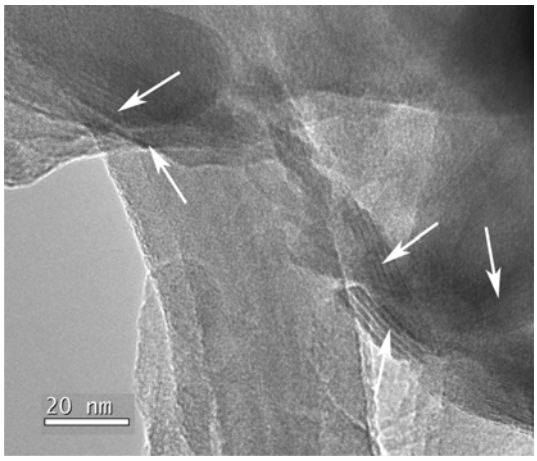

Figure 4. TEM image of MS10.

Figure 4 shows a TEM image of the MS10 composite hydrogel, MS platelets can be observed in the composite, which indicates that MS led to a better dispersion in the polymeric matrix without flocculation. This observation agrees with the FESEM results.

Effect of MS Content on Swelling Capacity. As shown in Figure 5, the swelling capacity of the hydrogel sharply increased with increasing the MS content, reached a maximum at 10 wt% (906 g/g), and then decreased with the further increase of MS content to 30 wt%. The greater enhancement of swelling capacity is due to the following reasons: (i) the polymer network can be improved and the network void for holding water can be regularly formed because MS

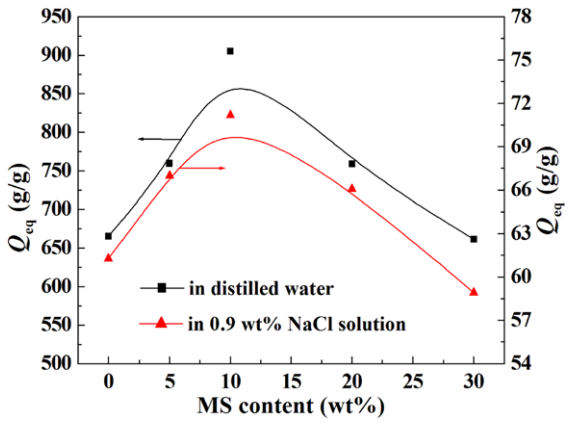

Figure 5. Effect of MS content on the swelling capacity of the composite hydrogel.

may participate in polymerization reaction; (ii) the existence of rigid MS in network structure prevented intertwining of polymeric chains and weakened the hydrogen-bonding interaction among hydrophilic groups. As a result, the physical crosslinking degree was decreased and the swelling capacity was increased; (iii) MS can ionize and generate lots of metal cations and [-SiO]$^-$ anionic groups when it contacting with water.[30] These ions not only increased the concentration of electrolyte in internal gel network and enhanced the osmotic pressure difference between gel network and swelling media, but also enhanced the repulsion among the negatively charged graft polymer chains and [-SiO]$^-$ groups. Thus, the swelling capacity was clearly enhanced. However, the excessive MS is physically filled in the gel network. This not only leads to the decrease of the hydrophilicity of the composite hydrogel, but also induces the block of the network voids for holding water. As a result, the swelling capacity decreased with the increase of the MS content above 10 wt%.

pH-Sensitive Properties. pH-sensitive properties of a hydrogel is especially important to its extended application such as drug-delivery system. As shown in Figure 6, the MS 10 composite hydrogel almost does not swell at pH 2.0, but its swelling capacity rapidly recovered when it was contacted with pH 7.4 solution. After the fully swollen gel was immersed in pH 2.0 solution again, the expanded gels may rapidly deswell and shrink, and an intriguing pulsatile and on-off switching pH-sensitive behavior was observed. This behavior can be ascribed to the fact that the -COO$^-$ groups of the hydrogel can convert to -COOH groups in pH 2.0 solutions, which strengthened the hydrogen bonding interaction among hydrophilic groups and increased the physical crosslinking degree. Thus, the swelling capacities of the hydrogels are low. However, when the pH value was increased to 7.4, the opposite process occurred. The hydrogen bonding interaction among hydrophilic groups was broken, and the electrostatic repulsion among polymer chains was

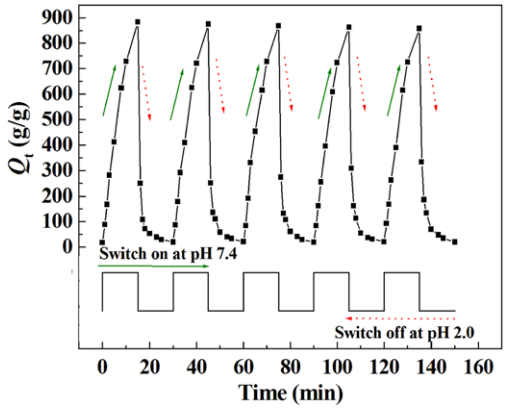

Figure 6. The On-Off switching behavior as reversible pulsatile swelling (pH=7.4) and deswelling (pH=2.0) of MS10 composite hydrogel. The time interval between pH changes is 15 min.

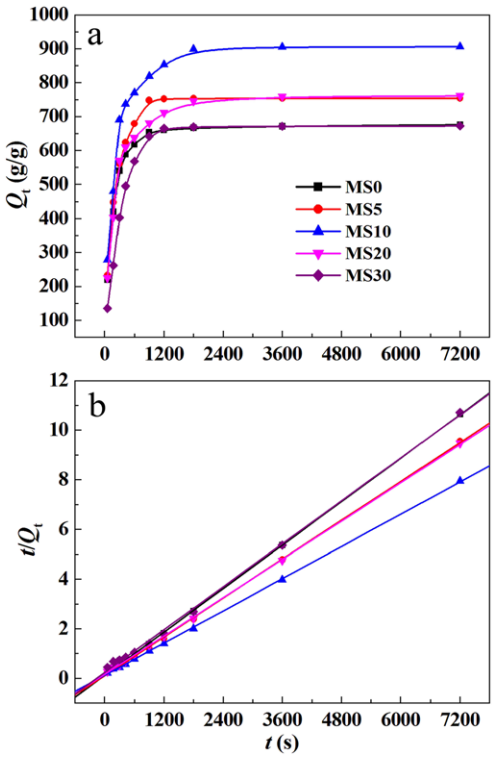

Figure 7. (a) Swelling kinetic curves of the composite hydrogels with various amounts of MS in distilled water; (b) plots of t/Q_t versus time t for each hydrogel.

increased, and so the hydrogels can swell more. After five swelling-deswelling (on-off) cycles between pH 7.4 and 2.0, the composite hydrogel still showed better sensitivity, which implies that the pH-sensitivity of the hydrogel are highly reversible.

Swelling Kinetics. Figure 7 shows the swelling kinetic curves of the hydrogels in distilled water. As can be seen, the swelling rate is faster at initial stage and then slowed down, until equilibrium state was reached within 900 s. For evaluating the kinetic swelling behaviors of the composite hydrogels, the Schott's pseudo-second order kinetic model was introduced and expressed as follows.[35]

$$t/Q_t = 1/K_{is} + (1/Q_\infty)t \quad (2)$$

Here, Q_t (g/g) is the swelling capacity of hydrogel at a given time t, Q_∞ (g/g) is the theoretical equilibrium swelling capacity, and K_{is} is the initial swelling rate constant (g/g·s). As shown in Figure 7(b), the graphs of t/Q_t versus t for both MS0 hydrogel and NaAlg-*g*-PNaA/MS composite hydrogels obtained straight lines with better linear correlation coefficient (> 0.99), which gives a direct revelation that the kinetic swelling process of the hydrogels obeys the Schott's theoretical model. By the slope and intercept of the lines, the kinetic parameters K_{is} and Q_∞ can be calculated (Table I). It can be noticed that the Q_∞ values are almost equal to the experimental values, and the K_{is} values for each

Table I. Swelling Kinetic Parameters for the Composite Hydrogels in Distilled Water

Samples	Q_{eq} (g/g)	Q_{∞} (g/g)	K_{is} (g/g·s)	R
MS0	665	676	9.0827	0.9999
MS5	760	769	9.6145	0.9998
MS10	905	926	8.2474	0.9998
MS20	765	774	6.3367	0.9999
MS30	662	675	4.3476	0.9993

hydrogel follows the order: MS5 > MS0 > MS10 > MS30. This result indicates the incorporation of moderate amount of MS obviously improved the swelling rate of the hydrogel, but the excessive addition of MS decreased it. This is because that MS may participate in the formation of 3D hydrophilic network and inhibit the intertwisting of graft polymer chains, which improved the network structure and the surface structure of the hydrogel, and thus contribute to the rapid penetration of water molecules into the hydrogel networks. But, the excess MS decreased the affinity of the hydrogel network with water molecules and block the network void for holding water, which decreased the dispersion rate of water molecules into hydrogel network.

Effect of Saline Solutions on the Swelling Behavior. The effect of saline solutions with different cations (Na^+, Ca^{2+} and Al^{3+}) and common anion (Cl^-) on the swelling capacity of the composite hydrogel was investigated (Figure 8). As can be seen, the swelling capacity degreased with increasing the concentration of external salt solutions, and the decreasing trend in multivalent cationic saline solutions is more obvious than in monovalent one. It can also be noticed that the swelling capacity in multivalent saline ($CaCl_2$ and $AlCl_3$) solution is almost close to zero at the concentration above 5 mmol/L, but can reach 296 g/g (5 mmol/L) and 226 g/g (10 mmol/L) in monovalent NaCl solution. The shrinkage of swelling capacity is because that the osmotic pressure difference (denoted as a driving force for swelling)

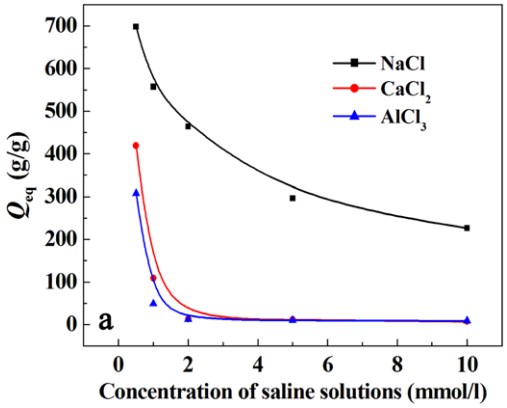

Figure 8. Effect of various saline solutions on the swelling behaviors of the MS10 composite hydrogel.

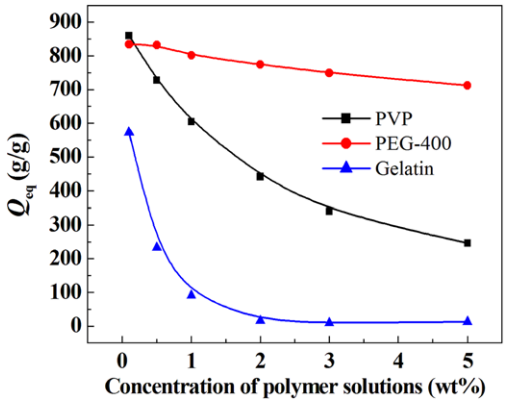

Figure 9. Effect of various polymer solutions on the swelling behaviors of the MS10 composite hydrogel.

between gel networks and the saline media was reduced and the screening effect of cations on negatively charged -COO^- groups was increased with increasing the saline concentration. In the solution of multivalent saline, the ionic sites of the hydrogel can complex with multivalent cations, which weakened the negative charges in polymeric chains and produces denser network by ionic crosslinking interaction. As a result, the expanding of polymeric network was restricted and the swelling capacity decreased more remarkably.

Effect of Polymer Solutions on the Swelling Behavior. The effects of saline and pH value of swelling media on the swelling capacity of hydrogels have been extensively investigated, but little attention was paid to explore the effect of various polymer solutions on swelling properties. In this section, the swelling behaviors of the composite hydrogel in PVP, PEG-400 and gelatin solutions were evaluated (Figure 9). As can be seen, with increasing the concentration of polymer solution, the swelling capacity of the composite hydrogel exhibited distinct change trends. With increasing the concentration of polymer solutions from 0.1 wt% to 5.0 wt%, the swelling capacity only lost about 14.7% in PEG-400 solution and 71.4% in PVP solution, but lost 97.9% in gelatin solution. For exploring the reason, the change of hydrophilic groups of the composite hydrogel before and after swelling in polymer solution was revealed by the FTIR spectra (Figure 10). It can be noticed that the characteristic absorption bands of gelatin at 1632 cm^{-1} appeared in Figure 10(b) and Figure 9(c) but shift to 1645 cm^{-1}. The characteristic absorption of MS10 at 1717 and 1573 cm^{-1} shifted to 1645 and 1554 after swelling in 5 wt% gelatin solution, indicating that gelatin existed in the hydrogel and combined with the -COOH groups of hydrogel by hydrogen bonding interaction. As can also be seen, the characteristic absorption bands of PVP at 1653, 1494, 1463, 1422 and 1289 cm^{-1} appeared in Figure 10(e) and 10(f) with different intensity, and shift to 1658, 1495, 1463, 1424 and 1292 cm^{-1}. The characteristic absorption of MS10 at 1717 and 1573 cm^{-1} shifted to 1724 and 1658 cm^{-1}, indicating that -COO^- groups

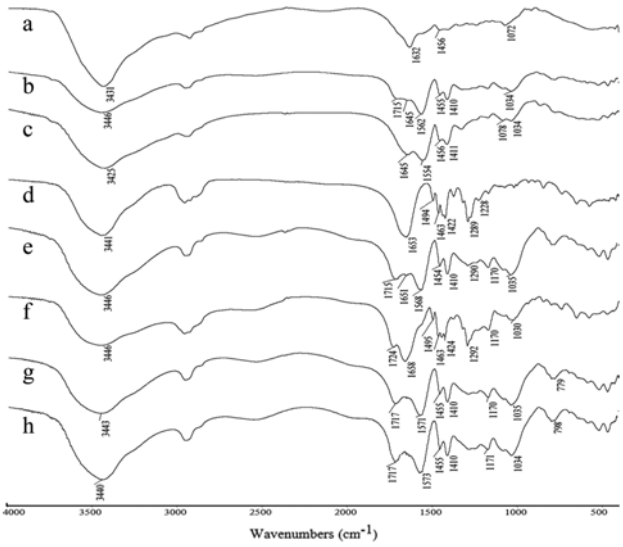

Figure 10. FTIR spectra of gelatin (a), MS10 composite hydrogel after swelling in 0.5 wt% (b) and 5 wt% (c) gelatin solutions, PVP (d), MS10 composite hydrogel after swelling in 0.5 wt% (e) and 5 wt% (f) PVP solution, MS10 composite hydrogel after swelling in 0.5 wt% (g) and 5 wt% (h) PEG-400 solution.

converted to -COOH groups at acidic condition (the pH values of 0.5 wt% and 5 wt% PVP solutions are 3.47 and 3.14, respectively) and the hydrogen bonding interaction occurred between -COOH groups and PVP. However, the FTIR spectra of MS10 composite hydrogel has no obvious change after swelling in PEG-400 solution, which reveals that no interaction occurred between the gel network and PEG-400 molecules.

Gelatin contains numerous -NH_2 and -COOH groups, which can form strong hydrogen bonding interaction with the -COOH of the composite hydrogel. After entering the gel network, the linear gelatin macromolecules may tangle with the graft polymer chains by the hydrogen bonding interaction among -COOH, -NH_2 and -OH groups, and the tangle degree increased with increasing gelatin concentration. As a result, the physical crosslinking degree was drastically increased and the gel network tends to collapse, the swelling capacity rapidly decreased. In PVP solution, the PVP molecules may also generate interaction with the -COOH groups of the hydrogel. With the concentration of PVP increasing to 5 wt%, the pH value of solution decreased from 3.8 to 3.2. The decrease of pH value not only increased the number of -COOH groups, but also decreased the negative charges on PVP molecules. The hydrogen bonding interaction increased with increased the PVP concentrations, more PVP molecules entered the network of hydrogel and intertwist with the graft polymer chains. The physical crosslinking increased and the swelling capacity of the hydrogel was reduced. However, PEG-400 molecules have almost no interaction with the hydrogel network, and so the swelling capacity has only little change. The small decrease of swelling capacity is mainly due to the decrease of solubility parameters of solution.

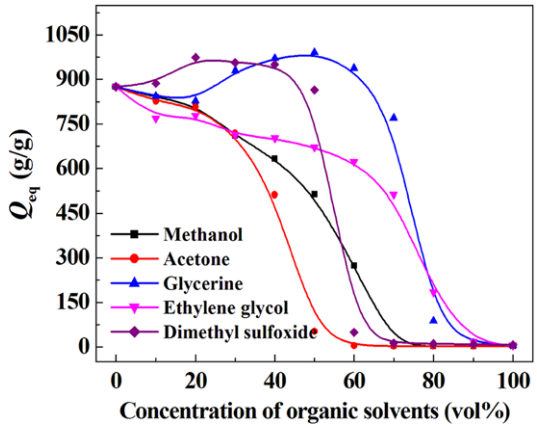

Figure 11. Swelling behaviors of the MS10 composite hydrogel in various hydrophilic organic solvents/water mixture solutions.

Effects of Hydrophilic Organic Solvents on the Swelling Behaviors. Effects of hydrophilic organic solvents on the swelling behaviors of the composite hydrogel have attracted great interests because of the intriguing gel phase transition and its smartness aspects.[36] Figure 11 shows the swelling curves of the composite hydrogel in the aqueous solution of methanol, acetone, glycerol, ethylene glycol and dimethyl sulfoxide (DMSO) at various concentrations. It can be clearly observed that the swelling capacity slowly decreased with increasing the concentration of methanol, acetone and ethylene glycol solution at the low concentration range (<40 vol% for methanol; <30 vol% for acetone; <60 vol% for ethylene glycol), but the gel rapidly deswells with increasing the concentration of methanol (≥40 vol%), acetone (≥30 vol%), ethylene glycol (≥60 vol%), DMSO (≥50 vol%) and glycerol (≥60 vol%) solutions, until the gel almost thoroughly collapsed at the concentration of 70 vol% for methanol, 60 vol% for acetone, 60 vol% for DMSO, 90 vol% for ethylene glycol and 90 vol% for glycerol. The solvent-induced swelling-loss of the hydrogels can be expressed by the Hildebrand equation (eq. (3)).[37]

$$\Delta H_m/(V_m \Phi_1 \Phi_2) = (\delta_1-\delta_2)^2 \quad (3)$$

where ΔH_m is the enthalpy change after mixing a polymer and a solvent, V_m is the whole volume of the solution, Φ_1 and Φ_2 are the volume fractions for the solvent and the polymer, δ_1 and δ_2 are the solubility parameters for the solvent and the polymer, respectively. It can be concluded from eq. (3) that the swelling capacity of a hydrogel is mainly dependent on its solubility in a given swelling media. As described previously, the δ value of the hydrogel is equal to the δ value of water (23.4 $(cal/cm^3)^{1/2}$). For a mixture solution, the solubility parameter (δ_{mix}) can be calculated using eq. (4).[37]

$$\delta_{mix} = \delta_1 \psi_1 + \delta_2 \psi_2 \quad (4)$$

where ψ_1 and ψ_2 are the volume fraction for the two components, and δ_1 and δ_2 are the solubility parameters of each component. The δ values of methanol, acetone, DMSO, ethylene glycol and glycerol are 14.5, 9.9, 14.5, 14.6 and 16.5 $(cal/cm^3)^{1/2}$, respectively, which is clearly smaller than 23.4 of water. Thus, the addition of methanol, acetone and ethylene glycol (poor solvent for the hydrogel) may induce the decrease of swelling capacity. It can also be calculated that the δ value for the hydrogel beginning to collapse is 18.95 $(cal/cm^3)^{1/2}$ for methanol, 18 $(cal/cm^3)^{1/2}$ for acetone, 18.95 $(cal/cm^3)^{1/2}$ for DMSO, 18.12 $(cal/cm^3)^{1/2}$ for ethylene glycol and 19.26 $(cal/cm^3)^{1/2}$ for glycerol. Besides solubility parameters, the dielectric constant of the solution directly affects the ionization degree of ionic groups, and then changes the difference of ion concentrations between gel network and external solution.[38] As a result, the swelling capacity can be affected. The dielectric constant of binary mixture solution can be calculated by eq. (5).

$$\varepsilon_{mix} = 78.54 \psi_1 + \varepsilon_2 \psi_2 \quad (5)$$

where ψ_1 and ψ_2 denote the volume fractions of water and organic solvents, respectively, and ε_2 represent the dielectric constants of organic solvents. The dielectric constants of water, methanol, acetone, DMSO, ethylene glycol and glycerol are 78.54, 33, 20.7, 47.2, 37 and 47 respectively. The addition of methanol, acetone or ethylene glycol certainly decreases the dielectric constants of the mixture solutions, and the dissociation of -COOH and $-COO^-$ groups was restrained, and so the swelling capacity also exhibits a similar decreasing tendency with increasing the concentration of methanol, acetone or ethylene glycol. In addition, DMSO and glycerol has relatively greater dielectric constant than the others, so the change of dielectric constant only shows little influence on the deswelling of the hydrogel.

However, a distinct trend was observed in the aqueous solutions of DMSO and glycerol in the concentration range from 0 to 50 vol% and from 0 to 60 vol%, respectively. The swelling capacity initially increased with increasing the concentration of DMSO and glycerol until the maximum swelling capacity was achieved at 20 vol% for DMSO and at 50 vol% for glycerol, and a similar trend was also observed in previous work.[39] The experiments were repeated for several times, and the "overflowing" behavior is reproducible. The "overflowing" behaviors can be attributed to the following reasons: in the aqueous solution of DMSO and glycerol, the additional hydrogen bonding interaction between the gel network and DMSO or glycerol molecules is stronger than the others. In aqueous solution of DMSO or glycerol, the DMSO or glycerol molecules may enter the gel network and form hydrogen bonding with the hydrophilic groups.[39] Thus, numerous DMSO molecules may reside in the interior of gel network. When the initial concentration of DMSO and glycerol solutions is lower than 50 and 60 vol%, respectively, the DMSO or glycerol concentration in interior gel network is higher than that in external solution (the DMSO and glycerol were denoted as a solute), and an additional osmotic pressure $\Delta\Pi_{org}$ was generated.[38] Under this condition, the comprehensive contribution of additional osmotic pressure $\Delta\Pi_{org}$ to enhance the swelling capacity is larger than the decreasing effect of the solubility parameter and dielectric constant on the swelling capacity. As a result, the swelling capacity was enhanced after adding moderate amount of DMSO or glycerol into aqueous solution. But the further increase of the external concentration of DMSO or glycerol leads to the disappearance of concentration difference of DMSO or glycerol, between gel network and external solution. Thus, the effect of the solubility parameter and dielectric constant becomes dominant, and the swollen gel rapidly collapsed when DMSO concentration is higher than 50 vol% and glycerol concentration is higher than 60 vol%.

Adsorption Properties of the Composite Hydrogels on Heavy Metal Ions. Besides excellent swelling properties, the composite hydrogels showed satisfactory adsorption performance on heavy metal ions. Figure 12 gives the equilibrium adsorption graphs of active carbon (AC), MS, MS5, MS10, MS20 and MS30 on Ni^{2+}, Cu^{2+}, Zn^{2+} and Cd^{2+} ions in aqueous solution. It can be observed that the equilibrium adsorption capacity of each absorbent follows the order MS5 (2.69 mmol/g for Ni^{2+}, 4.14 mmol/g for Cu^{2+}, 2.88 mmol/g for Zn^{2+} and 3.70 mmol/g for Cd^{2+}) > MS10 (2.28 mmol/g for Ni^{2+}, 3.99 mmol/g for Cu^{2+}, 2.60 mmol/g for Zn^{2+} and 3.68 mmol/g for Cd^{2+}) > MS20 (2.07 mmol/g for Ni^{2+}, 3.83 mmol/g for Cu^{2+}, 2.45 mmol/g for Zn^{2+} and 3.42 mmol/g for Cd^{2+}) > MS30 (2.80 mmol/g for Ni^{2+}, 1.76 mmol/g for Cu^{2+}, 2.21 mmol/g for Zn^{2+} and 3.11 mmol/g for Cd^{2+})>>AC (0.26 mmol/g for Ni^{2+}, 0.52 mmol/g for Cu^{2+}, 0.13 mmol/g for Zn^{2+} and 0.26 mmol/g for Cd^{2+})>

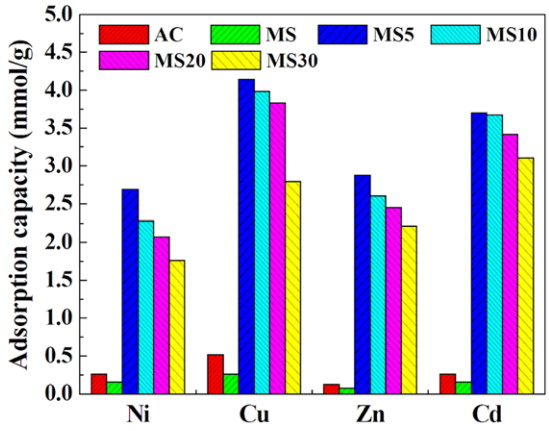

Figure 12. Adsorption capacity graphs of the composite hydrogels, active carbon and MS for heavy metal ions Ni^{2+}, Cu^{2+}, Zn^{2+} and Cd^{2+}, respectively.

MS (0.16 mmol/g for Ni^{2+}, 0.26 mmol/g for Cu^{2+}, 0.08 mmol/g for Zn^{2+} and 0.16 mmol/g for Cd^{2+}). The composite hydrogels with 5, 10, 20 and 30 wt% MS all showed higher adsorption capacity than AC and MS, which enhanced the adsorption amount on Ni^{2+}, Cu^{2+}, Zn^{2+} and Cd^{2+} ions by 10.4, 8.0, 23.0, and 14.3 folds in contrast to AC and 17.3, 16.0, 38.3 and 23.8 folds in contrast to MS, respectively. The composite hydrogels contain numerous $-COO^-$ groups, which can complex with heavy metal ions. The strong complexation interaction makes the composite hydrogel having relatively higher adsorption capacity than AC and MS that is mainly dependent on the physical adsorption.

Conclusions

As part of efforts to design and develop new kinds of environmentally friendly hydrogel materials with super-swelling and heavy metal ions adsorption characteristic and to reduce the excessive consumption of petroleum products, the biopolymer-based composite hydrogels were prepared by free-radical graft copolymerization among NaAlg, NaA and MS in the presence of initiator ammonium persulfate (APS) and crosslinker *N,N'*-methylene-*bis*-acrylamide (MBA). It was confirmed that NaA monomers have grafted onto NaAlg macromolecular chain, and MS participates in polymerization reaction. The introduction of MS clearly improved the surface morphologies and thermal stability, enhanced the swelling capacity and rate of the hydrogels. The composite hydrogel shows excellent on-off switching swelling characteristics between pH 2.0 and 7.2, which represents an intriguing pH-sensitive behavior and render the hydrogel potential as drug-delivery carrier. The swelling behaviors in various polymer solution revealed that the composite hydrogel rapidly deswell in gelatin solution, but only small deswelling in PEG-400 solution. The obvious deswelling behaviors were observed in DMSO/water and glycerol/water mixture solution, the composite hydrogel shows interesting "overflowing" swelling behavior, but no similar behavior was observed in other organic solvent/water mixture solution. Besides better swelling properties, the composite hydrogels showed excellent adsorption capacity on heavy metal ions Ni^{2+}, Cu^{2+}, Zn^{2+} and Cd^{2+}. The adsorption capacity of the composite hydrogels with 5, 10, 20 and 30 wt% MS enhanced the adsorption amount on Ni^{2+}, Cu^{2+}, Zn^{2+} and Cd^{2+} ions by 10.4, 8.0, 23.0, and 14.3 folds in contrast to AC and 17.3, 16.0, 38.3 and 23.8 folds in contrast to MS, respectively. Thus, the composite hydrogels based on renewable and biodegradable natural NaAlg and MS clay resources exhibited improved swelling capacity and rate as well as higher adsorption capacity for heavy metal ions, which can be used as promising water-manageable materials and as adsorbents for wastewater treatment.

Acknowledgement. The authors thank for jointly supporting by the National Natural Science Foundation of China (No. 20877077) and "863" Project of the Ministry of Science and Technology, P. R. China (No. 2006AA100215).

References

(1) H. Omidian and K. Park, in *Introduction to Hydrogels. Biomedical Applications of Hydrogels Handbook*, 2010, pp 1-16, DOI: 10.1007/978-1-4419-5919-5_1.
(2) M. R. Guilherme, A. V. Reis, A. T. Paulino, T. A. Moia, L. H. C. Mattoso, and E. B. Tambourgi, *J. Appl. Polym. Sci.*, **117**, 3146 (2010).
(3) M. Teodorescu, A. Lungu, P. O. Stanescu, and C. Neamtu, *Ind. Eng. Chem. Res.*, **48**, 6527 (2009).
(4) A. Das, V. K. Kothari, S. Makhija, and K. Avyaya, *J. Appl. Polym. Sci.*, **107**, 1466 (2008).
(5) K. S. V. Krishna Rao and C. S. Ha, *Polym. Bull.*, **62**, 167 (2009).
(6) J. M. Carvalho, M. A. Coimbra, and F. M. Gama, *Carbohydr. Polym.*, **75**, 322 (2009).
(7) M. Mahkam, N. Poorgholy, and L. Vakhshouri, *Macromol. Res.*, **17**, 709 (2009).
(8) G. Güçlü, E. Al, S. Emik, T. B. İyim, S. Özgümüş, and M. Özyürek, *Polym. Bull.*, **65**, 333 (2010).
(9) M. R. Guilherme, A. V. Reis, A. T. Paulino, A. R. Fajardo, E. C. Muniz, and E. B. Tambourgi, *J. Appl. Polym. Sci.*, **105**, 2903 (2007).
(10) M. Dalaran, S. Emik, G. Güçlü, T. B. İyim, and S. Özgümüş, *Polym. Bull.*, **63**, 159 (2009).
(11) H. Kaşgöz and A. Durmus, *Polym. Adv. Technol.*, **19**, 838 (2008).
(12) W. Kangwansupamonkon, W. Jitbunpot, and S. Kiatkamjornwong, *Polym. Degrad. Stab.*, **95**, 1894 (2010).
(13) J. K. Kim and Y. K. Han, *Macromol. Res.*, **16**, 734 (2008).
(14) K. Y. Lee and D. J. Mooney, *Chem. Rev.*, **101**, 1869 (2001).
(15) K. Lange, B. E. Rapp, and M. Rapp, *Anal. Bioanal. Chem.*, **391**, 1509 (2008).
(16) I. Šimkovic, *Carbohydr. Polym.*, **74**, 759 (2008).
(17) S. S. Ray and M. Bousmina, *Prog. Mater. Sci.*, **50**, 962 (2005).
(18) E. Al, G. Güçlü, T. B. İyim, S. Emik, and S. Özgümüş, *J. Appl. Polym. Sci.*, **109**, 16 (2008).
(19) Q. Z. Dai and J. F. Kadla, *J. Appl. Polym. Sci.*, **114**, 1664 (2009).
(20) W. B. Wang, J. P. Zhang, and A. Q. Wang, *Appl. Clay Sci.*, **46**, 21 (2009).
(21) A. Pourjavadi, A. M. Harzandi, and H. Hosseinzadeh, *Macromol. Res.*, **13**, 483 (2005).
(22) N. G. Kandile and A. S. Nasr, *Carbohydr. Polym.*, **78**, 753 (2009).
(23) M. R. Guilherme, A. V. Reis, S. H. Takahashi, A. F. Rubira, J. P. A. Feitosa, and E. C. Muniz, *Carbohydr. Polym.*, **61**, 464 (2005).
(24) M. H. Huang and M. C. Yang, *Polym. Adv. Technol.*, **21**, 561 (2010).
(25) M. R. Guilherme, T. A. Moia, A. V. Reis, A. T. Paulino, A. F. Rubira, L. H. C. Mattoso, E. C. Muniz, and E. B. Tambourgi,

Biomacromol., **10**, 190 (2009).
(26) R. Russo, M. Malinconico, and G. Santagata, *Biomacromol.*, **8**, 3193 (2007).
(27) A. Pourjavadi, M. S. Amini-Fazl, and H. Hosseinzadeh, *Macromol. Res.*, **13**, 45 (2005).
(28) A. Pourjavadi, H. Ghasemzadeh, and R. Soleyman, *J. Appl. Polym. Sci.*, **105**, 2631 (2007).
(29) R. Meena, M. Chhatbar, K. Prasad, and A. K. Siddhanta, *Polym. Int.*, **57**, 329 (2008).
(30) J. Li, P. Y. Zhang, Y. Gao, X. G. Song, and J. H. Dong, *Environ. Sci. Technol. (China)*, **31**, 63 (2008).
(31) A. Li, A. Q. Wang, and J. M. Chen, *J. Appl. Polym. Sci.*, **92**, 1596 (2004).
(32) J. H. Wu, J. M. Lin, G. Q. Li, and C. R. Wei, *Polym. Int.*, **50**, 1050 (2001).
(33) B. L. Yao, C. H. Ni, C. Xiong, C. P. Zhu, and B. Huang, *Bioprocess Biosyst. Eng.*, **33**, 457 (2010).
(34) Y. H. Huang, J. Lu, and C. B. Xiao, *Polym. Degrad. Stab.*, **92**, 1072 (2007).
(35) H. Schott, *J. Macromol. Sci. B*, **31**, 1 (1992).
(36) M. Shibayama and T. Tanaka, *Adv. Polym. Sci.*, **109**, 1 (1993).
(37) J. W. Chen and J. R. Shen, *J. Appl. Polym. Sci.*, **75**, 1331 (2000).
(38) Y. Liu, J. J. Xie, M. F. Zhu, and X. Y. Zhang, *Macromol. Mater. Eng.*, **289**, 1074 (2004).
(39) K. Kabiri, M. J. Zohuriaan-Mehr, H. Mirzadeh, and M. Kheirabadi, *J. Polym. Res.*, **17**, 203 (2010).